The origins of spontaneous grain refinement in deeply undercooled metallic melts

2016 IOP Conf. Ser.: Mater. Sci. Eng. 117 012054

(http://iopscience.iop.org/1757-899X/117/1/012054)

The origins of spontaneous grain refinement in deeply undercooled metallic melts

A M Mullis[a], E G Castle[b] and R F Cochrane[c]
Institute for Materials Research, University of Leeds, Leeds LS2-9JT, UK

E-mail: [a] a.m.mullis@leeds.ac.uk, [b] pm07egc@leeds.ac.uk, [c] r.f.cochrane@leeds.ac.uk

Abstract. Spontaneous grain refinement in undercooled metallic melts has been a topic of enduring interest within the solidification community since its discovery more than 50 years ago. Here we present a comparative study of the solidification microstructures and velocity-undercooling behaviour in two dilute Cu-Ni alloys (3.98 & 8.90 wt.% Ni), which have been undercooled by a melt encasement (fluxing) method. Cu-3.98 wt.% Ni shows grain refinement at both low and high undercooling, with a dendritic growth regime separating the two grain refined regions. Within the grain refined region dendritic fragments are clearly evident in the centres of the refined grains and on the surface of the undercooled droplet, suggesting a dendritic fragmentation mechanism. Cu-8.90 wt.% Ni displays also grain refinement at both high and low undercoolings. In the low undercooling grain refined region the samples display curved grain boundaries with a dendritic substructure that extends across grains, indicative of a recovery and recrystallisation mechanism. Conversely, prior to the onset of the high undercooling grain refinement transition extensive regions of dendritic seaweed are observed, suggesting that it is remelting of a dendritic seaweed that gives rise to this structure. Consequently, in two closely related Cu-based systems we have strong microstructural evidence for the operation of all three mechanisms currently considered to give rise to grain refinement. This may help to resolve the grain refinement controversy, although it remains to be determined what factors determine which mechanism operates in any given system.

1. Introduction

A long-standing problem with regard to the dendritic solidification of metals has been that of spontaneous grain refinement in undercooled melts, first reported in pure Ni by Walker [1]. At a well defined undercooling, ΔT^*, Walker observed an abrupt transition from a coarse columnar, to a fine equiaxed, structure with a reduction in grain size of at least one order of magnitude. This effect has subsequently been identified in other pure metals [2, 3, 4] and in a range of alloy systems [5, 6, 7, 8, 9], in which a more complex evolutionary sequence is often observed. At low undercooling an initially columnar growth pattern is observed which gives way to an equiaxed grain structure as the undercooling is increased beyond a critical value, ΔT_1^*. At yet higher undercooling a second region of columnar growth is observed which, in most of systems, is replaced by a second region of equiaxed growth at still higher undercooling, ΔT_2^*. In many systems the onset of spontaneous grain refinement is observed to be simultaneous with a discontinuity in the velocity-undercooling curve [2].

The origins of the effect are controversial. Early theories suggested a range of mechanisms including nucleation ahead of the solidification front induced by the pressure pulse associated with solidification [1], recrystallisation, either during or immediately after solidification [10, 11], or the role

of minor solute additions [12, 13, 14]. However, more recent theories have tended to invoke fragmentation of the primary crystal, either during [15, 16], or immediately post-recalescence [17, 18]. The model that has perhaps achieved the most currency is that of Schwarz *et al*. [17, 18]. The model postulates that two characteristic timescales can be defined. The first is the break-up time, τ_{bu}, which is the time required for fragmentation of side branches due to remelting and Rayleigh instability. This is a monotonic function of the dendrite tip radius, with small radii giving short breakup times. The second timescale is the plateau time, τ_{pl}, which is the time the melt remains at, or around, the melting temperature during recalescence and is determined by the macroscopic heat extraction rate. The theory postulates that grain refinement occurs when $\tau_{bu} < \tau_{pl}$, which corresponds to the tip radius, ρ, being below some critical value, ρ^*, determined by the heat extraction rate. The original analysis was performed in the framework of the LKT model [19] for prediction of ρ, wherein the model appears to offer a natural explanation for grain refinement in both pure metals and alloys, although similar results can now be obtained using the more physically justifiable microscopic solvability theory [20].

An alternative mechanism for grain-refinement has been postulated in which a tip-splitting instability at the dendrite tip leads to the growth of an unstable 'dendritic seaweed' structure, which subsequently remelts to give the observed grain-refinement. This is supported the observation, in deeply undercooled ultra-high purity Cu, of a 'frozen in' seaweed morphology [21] above a critical undercooling, which resulted in a discontinuity in the velocity-undercooling curve identical in nature to that observed in spontaneous grain refinement [22].

In this paper we present the results of a microstructural investigation into the solidification of two closely related alloys (Cu- 3.98 wt.% Ni and Cu- 8.90 wt.% Ni) from their deeply undercooled melt. Both alloys show a variety of growth morphologies, including grain refinement, but subtle variations in the morphologies may yield important insights into the origin of spontaneous grain refinement.

2. Experimental method

High purity, 99.999% metals basis, Cu and Ni powders, of 100 and 120 mesh respectively, were weighed, mixed and compacted into pellets at nominal compositions close to Cu- 5 wt.% Ni and Cu-10 wt.% Ni. These were subsequently arc-melted together under an inert argon atmosphere. X-ray diffraction (XRD) patterns obtained from the alloys confirmed that a sufficient degree of homogeneity had been achieved and indicated the presence of a small amount of NiO. The composition of the as-solidified master alloys, accounting for any mass loss during preparation, was confirmed by Inductively Coupled Plasma – Optical Emission Spectroscopy (ICP-OES) analysis as Cu- 3.98 wt.% Ni and Cu-8.90 wt.% Ni. Prior to the conduct of undercooling experiments 5-7 mm pieces of the master alloy were ultrasonically cleaned in a warm aqueous solution of ammonium peroxodisulphate.

Undercooling experiments were carried out within a stainless steel vacuum chamber, evacuated to 10^{-5} mbar and backfilled to 500 mbar with N_2 gas. Samples were heated in fused silica crucibles by induction heating of a graphite susceptor, contained within an alumina radiation shield. In order to reduce the number of potential heterogeneous nucleation sites, the droplets were isolated from the crucible walls by suspension in a dewatered 40% Na_2SiO_3 – 60% B_2O_3 glass flux. The sample was visible throughout the experiment via a glass viewing window in the vacuum chamber and slots cut into the susceptor and alumina shield. High speed digital imaging (up to 15 000 fps) of the sample was used to make *in-situ* growth velocity measurements of the recalescence front.

Samples were subjected to repeated heating and cooling cycles, in which they were superheated to around 130 K above the liquidus temperature and held at this temperature for 15 minutes, ensuring complete melting and encasement of the sample and removal of gas bubbles from the flux. Samples were then slowly cooled through the liquidus at an average rate of 10 K/min. Temperature was monitored by means of an r-type thermocouple positioned at the base of the crucible. Solidification was allowed to nucleate spontaneously as this was found to occur naturally over a wide range of undercoolings and ensures that solidification proceeds from a single nucleation point. Further details of the experimental procedure are given in [23].

Samples, undercooled by varying amounts, were sectioned and mounted in Bakelite. Since growth proceeds radially outwards from the nucleation point, droplets with evident nucleation points could be sectioned with a well-defined orientation relative to their growth direction. To assess the interior microstructure of the droplets they were then polished and etched using an aqueous solution of ammonium persulphate. Microstructural analysis was by means optical microscopy (Olympus BX51 microscope), SEM secondary-electron imaging (Carl Zeiss EVO MA15 SEM) and XRD pole figure analysis (Phillips/PanAlytical diffractometer).

3. Results

The measured velocity undercooling behaviour for the two alloys is shown in figure 1. The same general trend is apparent in both cases. For low undercooling there is a relatively slow increase in growth velocity In this region a power-law fit to the data (not shown) indicates that, to a good approximation, the velocity increases as $(\Delta T)^2$. Beyond a critical undercooling, for which our best estimate is ΔT = 192 K ($v \approx 31$ m s^{-1}) for Cu- 3.98 wt.% Ni and ΔT = 204 K ($v \approx 29$ m s^{-1}) for Cu-8.90 wt.% Ni, there is a discontinuity in the velocity-undercooling curve, with the velocity increasing much more rapidly at higher undercooling. Where this has been observed previously it is normally indicative of either a change in dendrite growth direction, which in other Cu alloys has been from <100> to <111> [24], or a transition from growth controlled by solute diffusion to growth controlled by thermal diffusion as a result of solute trapping (see e.g. [25, 26] relating to Ni-B and Ni-Zr respectively). The microstructure determined from the resulting as-solidified samples is also summarised in figure 1.

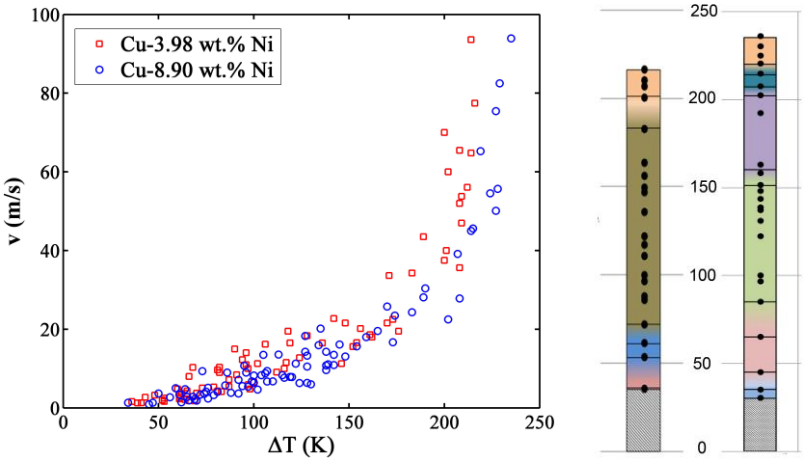

Figure 1. Velocity ΔT curves for the dilute Cu-Ni alloys investigated in this study. Also shown summary of the structures observed for the 3.98 (left) and 8.90 (right) alloys – Grain refined, low ΔT (pink); dendritic, low ΔT (light blue); mixed orientation (khaki); 8-fold dendritic (pale green); 6-fold dendritic (purple); dendritic (dark blue), grain refined (orange).

For ΔT < 35 K it is difficult to nucleate solidification of the flux encased droplet and consequently microstructure determination has not been possible. At ΔT = 35 K the Cu- 3.98 wt.% Ni already displays a grain refined microstructure, although on the assumption that growth at equilibrium is dendritic we assume that there is a low undercooling dendritic → grain refined transition but that this is located in the inaccessible region of very low undercoolings. Conversely, in the Cu-8.90 wt.% Ni alloy a coarse grained dendritic structure is observed up to undercoolings of 45 K, with a grain refined structure being obtained thereafter. These low undercooling grain refined regions persist up to undercoolings of 53 K and 85 K for the low and high Ni alloys respectively.

In both alloys this is then followed by an extended region in which dendrites with a variety of growth orientations are observed. In Cu- 3.98 wt.% Ni this begins with a region in which the dominant microstructure is for the droplet to comprise a single grain formed from a <100>-oriented dendrite with a strong orthogonality being observed between the primary and secondary arms. However, above ΔT = 72 K, and up to at least ΔT = 148 K, this gives way to a region in which the dendrites exhibit features of mixed-orientation growth; with secondary arms growing at both orthogonal and non-orthogonal angles to the primary trunk, some of which also appear to show twinning about the {111} plane. At undercoolings above 184 K this is replaced by a grain refined structure.

In contrast, in the Cu-8.90 wt.% Ni alloy, a much clearer transition in growth direction occurs. Above 85 K undercooling the grain refined structure gives way to dendritic growth with a clear 8-fold structure. This persists up to ΔT = 155 K, beyond which, and up to ΔT = 205 K, the dendrites adopt a 6-fold symmetry. Intermixed with these dendritic structures are regions of 'dendritic seaweed'. These 'seaweed' regions are bound by the dendrites and evolve from a diverging split primary branch, whose inner secondary branches have undergone multiple tip-splitting. In some cases, orthogonal outer secondary branches are observed to have grown from the split primary branches. In these cases, the seaweed growth is observed to terminate in an array of parallel <100> type dendrites. Finally, at very high undercooling a region of coarse, 4-fold symmetric, dendritic growth is observed up to undercoolings of 220 K, which finally gives way to a grain refined structure which is observed up to the highest undercoolings attained.

There are also significant differences in the morphologies observed in the grain refined regions. Figure 2a shows the typical microstructure observed in the Cu- 3.98 wt.% Ni alloy at low undercooling. Within the centre of the droplet, a large grain structure consisting of small subgrains is observed. Fragmented dendrite 'cores' are evident, with the low-angle subgrain boundaries most likely formed due to the slight misorientations between them. A surface micrograph (not shown) reveals that dendrite fragments which appear to exhibit secondary arms at 90° to the primary; suggesting that normal, <100>-oriented growth took place initially. The {200} pole figure taken from this sample indicates the presence of at least three unrelated grains, confirming the discontinuity of the substructure between them. The low undercooling region of grain refinement in this alloy appears therefore to take place via the fragmentation of <100>-oriented dendrites.

In contrast, in the low undercooling grain refined region in the Cu- 9.80 wt.% Ni alloy there appear to be large parent grains consisting of numerous small sub-grains. This is indicated by the difference in contrast between large areas, as shown in the top image of figure 2b - an optical micrograph of a sectioned, polished and etched sample which has been undercooled by ΔT = 65 K prior to solidification. The existence of curved grain boundaries suggests that grain boundary migration has taken place, whilst the DIC micrograph of the same sample (figure 2b bottom) appears to show that the coarse dendritic segregation pattern extends across the grain boundaries. The {200} pole figure plot taken from a randomly-oriented section of this sample exhibits only three sharp poles related to one another through 90º angles, confirming that the dendritic substructure is continuous throughout. This is consistent with the recrystallisation mechanism associated with the low undercooling region of grain refinement observed in many alloys [10, 11].

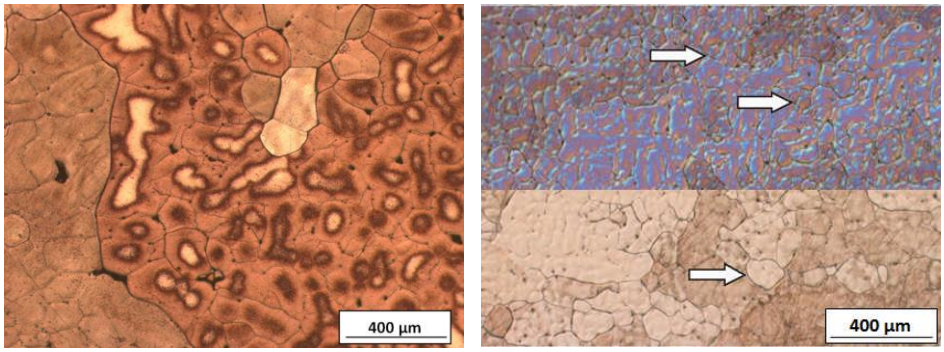

Figure 2. Grain refined microstructure of (a-left) Cu-3.98 wt.% Ni alloy (b-right) Cu-8.90 wt.% Ni alloy in the low undercooling regime. (a) shows clear evidence of dendrite fragmentation, (b) shows evidence of recrystallisation, indicated by curved grain boundaries and a substructure which is continuous across grains. This is particularly evident under DIC (top part of image).

For the Cu- 3.98 wt.% Ni alloy, grain refinement in the high undercooling regime also appears to proceed via a dendrite fragmentation mechanism. A surface microstructure, obtained from a droplet undercooled by ΔT = 216 K is shown in figure 3a. A fragmented dendrite structure can be seen; with

each fragment constituting a single grain. The interior microstructure (not shown) appears to show a dendritic substructure that traverse some, but not all, of the grain boundaries. The {111} pole figure displays numerous random, unrelated sets of poles, confirming the presence of a large number of randomly oriented grains. The morphology of these dendrites is unclear, making it difficult to determine the character of the original growth structure. However, the velocity data, and in particular the fact that grain refinement occurs only on the high velocity side of the discontinuity in the velocity-undercooling curve, suggests a <111> orientation. It therefore appears that the high undercooling region of grain refinement in this alloy arises from the fragmentation of dendrites, possibly with a <111> growth direction.

A different morphology is observed in the Cu- 8.90 wt.% Ni alloy at the highest undercoolings achieved, wherein the grain structure transitions from large elongated grains to fine equiaxed grains. This is confirmed by the {111} pole figure (figure 3b) which contains a large number of poles which are mostly confined to one half of the plot, indicating the presence of a number of individual grains, yet with overall directionality still existing. The small equiaxed grains appear devoid of any substructure. However, the substructure in areas which are not grain refined (where large elongated grains are observed) is distinctly dendritic seaweed-like in character, as shown in figure 3b. Here, we appear to be observing an intermediate stage in the spontaneous grain refinement process, in which it looks like the growth of dendritic seaweed is the precursor structure.

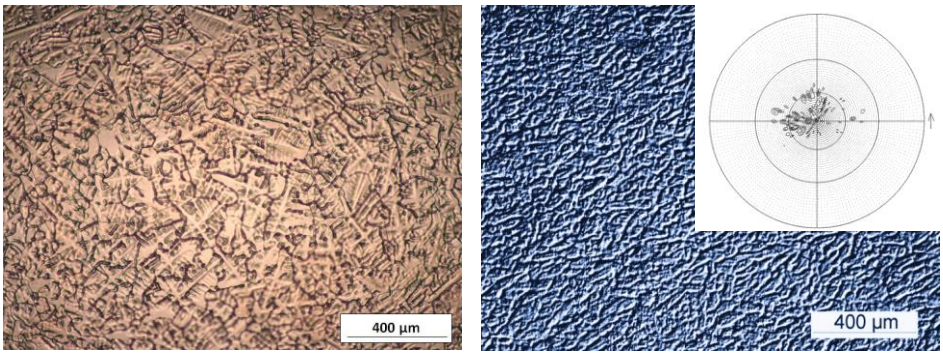

Figure 3. Grain refined microstructure of (a-left) Cu-3.98 wt.% Ni alloy (b-right) Cu-8.90 wt.% Ni alloy in the high undercooling regime. (a) shows clear evidence of dendrite fragmentation in the through focused image of the droplet surface, (b) shows extensive evidence of seaweed growth just prior to full grain refinement with {111} pole figure inset.

4. Discussion

Three distinct grain refinement mechanisms have been identified in the two closely related alloys studied here. Firstly, spontaneous grain refinement in the low-Ni alloy appears to be consistent with the model of Schwarz et al. [17], since two grain refinement transitions are observed to arise from the fragmentation of dendrites. At low undercooling grain refinement appears to occur from the fragmentation of refined <100> dendrites and, following an orientation transition, from the fragmentation of refined <111> dendrites at high undercooling.

A second grain refinement mechanism of recrystallisation has then been observed at low undercooling in the high-Ni alloy, consistent with a number of other reports [10, 11]. The difference between the fragmentation mechanism observed in the low-Ni alloy and the recrystallisation mechanism observed in the high-Ni alloy appears to arise from the difference in the original growth structure. In the low-Ni alloy, stable <100>-oriented growth is observed well beyond the first grain refinement transition, suggesting that the precursor in this case is <100> dendrites; in which case the greatest driving force for grain refinement seems to be the fragmentation of these dendrites following a gradual scale refinement. However, in the high-Ni alloy, there is an abrupt transition from the grain refined to the mixed-orientation regime, suggesting that the two regimes may coincide. Thus, the precursor to grain refinement in this instance would be mixed orientation dendrites; the presence of

which most likely indicates the existence of a high dislocation density, thereby providing sufficient driving force for a recovery/recrystallisation process in place of refinement and fragmentation.

Finally, the remelting and fragmentation of a seaweed precursor appears to be the most likely mechanism for spontaneous grain refinement at high undercooling in the high-Ni alloy; in line with that proposed by Mullis et al. [16]. In order to understand why seaweed is observed for the high Ni alloy only, a consideration of the effect of Ni content is required. Since the addition of more Ni to Cu shifts the mixed orientation regime to lower undercoolings (with respect to the first grain refinement transition), and since this facilitates a transition to seaweed growth, it is suggested that the addition of Ni changes the balance between the capillary and kinetic anisotropies, an idea supported by the work of Haxhimali et al. [27] and Dantzig et al. [28]. In particular, orientation selection maps produced by Haxhimali et al. showed both Cu and Ni being very close to the <100>-<110> orientation boundary.

5. Conclusions

Spontaneous grain refinement has been a long standing and contentious issue in the solidification of deeply undercooled melts. A number of mechanisms have been proposed which plausibly account for this phenomenon, including recovery and recrystallisation, fragmentation of dendrites and growth and subsequent fragmentation of a dendritic seaweed. A comparative study on the solidification of two closely related Cu-Ni alloys has revealed that under varying conditions all three mechanisms appear to operate, perhaps explaining the long standing confusion over the origins of the phenomenon.

6. References

[1] Walker J L 1959 *The Physical Chemistry of Process Metallurgy* (New York: Interscience).
[2] Wilnecker R, Herlach D M and Feuerbacher B 1989 *Phys. Rev. Lett.* **62** 2707.
[3] Battersby S E, Cochrane R F and Mullis A M 1999 *J. Mater. Sci.* **34** 2049.
[4] Dragnevski K, Cochrane R F and Mullis A M 2004 *Mater. Sci. Eng. A*, **375-377** 479.
[5] Battersby S E, Cochrane R F & Mullis A M 2000 *J. Mater. Sci.* **35** 1365.
[6] Zhang T, Liu F, Wang H F, Yang G C 2010 *Scripta Mater.* **63** 43.
[7] Li J F, Zhou Y H and Yang G C 2000 *Mater. Sci. Eng. A* **277** 161.
[8] Li J F, Jie W Q, Y and G C and Zhou Y H 2002 *Acta Mater.* **50** 1797.
[9] Wang N, Gao J R and Wei B 1999 *Scripta Mater.* **41** 959.
[10] Southin R T and Weston G M 1973 *J. Aust. Inst. Met.* **18** 74.
[11] Ovsiyenko D E, Maslov V V and Dneprenko V N 1979 *Russ. Met.* **6** 124.
[12] Jones B L and Weston G M 1970 *J. Aust. Inst. Met.* **15** 167.
[13] Jones B L and Weston G M 1970 *J. Aust. Inst. Met.* **15** 189.
[14] Powell G L F and Hogan L M 1969 *Trans. AIME* **245** 407.
[15] Mullis A M and Cochrane R F 1997 *J. Appl. Phys.* **82** 3783.
[16] Mullis A M and Cochrane R F 1998 *J. Appl. Phys.* **84** 4905.
[17] Schwarz M, Karma A, Eckler K and Herlach D M 1994 *Phys. Rev. Lett.* **73** 1380.
[18] Karma A 1998 *Int. J. Non-equilibrium Processing* **11** 201.
[19] Lipton J, Kurz W and Trivedi R 1987 *Acta Metall.* **35** 957.
[20] Alexandrov D V and Galenko P K 2013 *Phys. Rev. E* **87** 062403.
[21] Dragnevski K, Cochrane R F and Mullis A M 2002 *Phys. Rev. Lett.* **89** 215502.
[22] Mullis A M and Cochrane R F 2001 *Acta Mater.* **49** 2205.
[23] Castle E G, Mullis A M and Cochrane R F 2014. *Acta Mater.* **66** 378.
[24] Dragnevski K, Mullis A M and Cochrane R F 2004 *Metall. Mater. Trans. A* **35A** 3211.
[25] Eckler K, Herlach D M and Aziz M J 1994 *Acta Metall. Mater*. **42** 975.
[26] Galenko P K, Reutzel S, Herlach D M, Danilov D and Nestler B 2007 *Acta Mater*. **55** 6834.
[27] Haxhimali T, Karma A, Gonzales F, Rappaz M 2006 *Nat. Mater.* **5** 660.
[28] Dantzig J A, Napoli P D, Friedli J, Rappaz M. 2013 *Metall. Mater. Trans. A* **44** 5532.